IEEE Photonics Journal
An IEEE Photonics Society Publication

Open Access

Analysis of InGaN-Delta-InN Quantum Wells on InGaN Substrates for Red Light Emitting Diodes and Lasers

Volume 13, Number 1, February 2021

Bryan Melanson
Cheng Liu
Jing Zhang

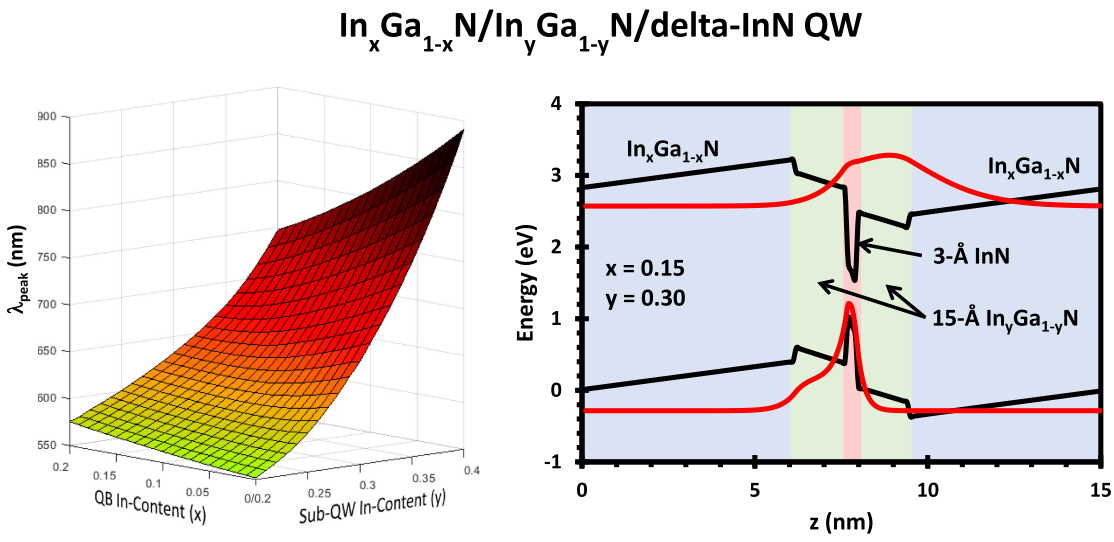

DOI: 10.1109/JPHOT.2021.3053484

Analysis of InGaN-Delta-InN Quantum Wells on InGaN Substrates for Red Light Emitting Diodes and Lasers

Bryan Melanson,[1] **Cheng Liu**,[1] **and Jing Zhang**[2]

[1]Microsystems Engineering Department, Rochester Institute of Technology, Rochester, NY 14623 USA
[2]Electrical and Microelectronic Engineering Department, Rochester Institute of Technology, Rochester, NY 14623 USA

DOI:10.1109/JPHOT.2021.3053484
This work is licensed under a Creative Commons Attribution 4.0 License. For more information, see https://creativecommons.org/licenses/by/4.0/

Manuscript received November 13, 2020; revised January 15, 2021; accepted January 19, 2021. Date of publication January 21, 2021; date of current version February 8, 2021. This work was supported in part by National Science Foundation under Award No. ECCS 1751675. Corresponding authors: Bryan Melanson; Jing Zhang (e-mail: bcm9356@rit.edu; jzeme@rit.edu).

Abstract: Modern multi-color RGB micro-light emitting diode (μLED) displays and digital micro-mirror laser projectors often require the use of both III-V and III-Nitride material systems for different pixel/laser colors. This is due primarily to the conventionally low efficiencies of red emitters based on the InGaN materials system, which is used to create green and blue emitters for RGB displays. The main challenges for InGaN red emitters are the quantum confined stark effect (QCSE) and the difficulty of incorporating high In-content into the active region. In this work, InGaN/InGaN/delta-InN quantum wells (QWs) on InGaN substrates are proposed and demonstrated to show significant enhancement in electron-hole wavefunction overlap (Γ_{e_hh}) and spontaneous emission radiative recombination rate (R_{sp}) in the red emission regime. Analysis of InGaN/InGaN/delta-InN QWs with InGaN barriers emitting at 630 nm was performed using a self-consistent six-band $k \cdot p$ formalism. The Γ_{e_hh} was shown to increase by more than 230% compared to an InGaN/InGaN QW emitting at 630 nm, leading to significant increases in R_{sp} and internal quantum efficiency (η_{IQE}). With growth of InN monolayers on InGaN now readily achievable, this novel active region design could pave the way for high-efficiency, native red-emitting InGaN LEDs and lasers.

Index Terms: LED, GaN, InGaN, delta-InN, red-emission, wavefunction, spectra, gain, laser.

1. Introduction

InGaN quantum well (QW) light emitting diodes (LEDs) and lasers have seen a significant increase in utilization over the past decade thanks to substantial increases in efficiency. InGaN LEDs are used extensively in industrial, commercial, and residential lighting applications as well as in emerging display technologies for μLED alternate reality (AR) and virtual reality (VR) headset displays, while InGaN laser diodes are used in digital micro-mirror device (DMD) laser projectors and are desirable for wafer level integration with silicon photonics [1]–[3]. While blue LEDs have been very well optimized over the past decade, often boasting external quantum efficiencies (η_{EQE}) greater than 85%, InGaN LEDs and lasers emitting at longer wavelengths still struggle to match the efficiencies of their blue counterparts, making it difficult to fabricate high-efficiency, high-brightness

red emitters for lighting, display, and laser applications [4]–[9]. Consequently, μLED displays often rely on AlInGaP for red-emitting pixels, which complicates the fabrication process and increases manufacturing costs [10]. Red lasers using InGaN QWs as the gain medium have not yet been achieved, and as a consequence InGaN quantum dot lasers are instead used in applications which require compact, high-efficiency RGB laser diodes, such as DMD laser projectors [11], [12]. The low η_{EQE} of red-emitting InGaN QWs can be attributed to the difficulty of incorporating high In-content layers into the active region, as well as the large internal electrostatic fields which exist within GaN/InGaN QWs, which can be on the order of 1–5 MV/cm [13], [15]. These internal electric fields serve to confine the electron and hole wavefunctions to the edges of the QW, reducing the electron-hole wavefunction overlap (Γ_{e_hh}) which in turn reduces the spontaneous emission radiative recombination rate (R_{sp}). Several techniques have been proposed and examined as means to alleviate the electron-hole wavefunction separation within GaN/InGaN QWs emitting at shorter wavelengths to address the quantum-confined Stark effect (QCSE), including use of non-polar InGaN [16], staggered InGaN QWs [17], [18], strain-compensated InGaN QWs [19], and type-II InGaN QWs [20], [21], as well as AlGaN-delta-GaN QWs [22], [23] and InGaN-delta-InN structures [24]. However, there have been very few studies performed on promising solutions for red emitters based on the InGaN materials system, which are of great importance for μLED displays, laser diodes, and other solid state lighting applications.

While staggered InGaN QWs have been shown to offer improved Γ_{e_hh} when compared to GaN/InGaN QWs, this enhancement becomes less pronounced in the red emission regime around 630 nm [17], [18]. Structures that incorporate an ultrathin delta-InN layer at the center of an InGaN QW have been shown to be more effective at maintaining high Γ_{e_hh} and high R_{sp} at green and red wavelengths [24]. In these structures, the peak emission wavelength can be roughly tuned by varying the thickness of the delta-InN layer [24]. The use an InN delta-layer within an InGaN QW has also been shown to enhance Γ_{e_hh} at longer wavelengths within the red emission regime [24], in contrast to other approaches, which suffer from decreasing Γ_{e_hh} as the emission wavelength is increased [17], [23]. Recent advances in epitaxial growth of InN make this a feasible approach for high volume manufacturing of epi-stacks incorporating InN delta-layers [25], [26]. While delta-InN structures have been shown to produce more efficient red emission, all existing studies have focused on InGaN-delta-InN QWs with GaN quantum barriers (QBs) grown on GaN substrates. The InN and high In-content InGaN epi-layers required for InGaN-delta-InN QWs have a much larger lattice constant than GaN, leading to formation of high-strength piezoelectric polarization electric fields within the QW which reduce Γ_{e_hh}. To solve this issue, the use of InGaN substrates has been proposed as a means to reduce lattice mismatch induced piezoelectric electric field intensity in the QW [27], [30]. Growth of thick InGaN layers on sapphire and GaN substrates has been well-demonstrated [31], [39], with these thick InGaN layers serving as growth templates for InGaN LED epi-stacks. However, InGaN QBs must be used in these structures, and suffer from low carrier injection efficiency due to reduced QB height. To resolve these issues and produce the most efficient red-emitting InGaN QW, we propose the use of an InGaN-delta-InN QW with an InGaN growth substrate, which can be used to reduce the piezoelectric electric field intensity while maintaining high carrier injection efficiency.

Here, we investigate an InGaN-delta-InN QW on an InGaN substrate (hereafter denoted as an $In_xGa_{1-x}N/In_yGa_{1-y}N$/delta-InN QW where x represents the In-content in the barrier/substrate and y the In-content in the sub-QW region) which addresses the QCSE and improves R_{sp} with greatly enhanced wavelength tunability in the red regime. In contrast to structures investigated in prior works [24], [27]–[30], our structure combines an InGaN-delta-InN QW active region with an InGaN substrate for the first time. The InGaN substrate, which is fully relaxed and possesses no internal strain itself, has same In-content as the QB regions, serves to reduce the lattice mismatch between epitaxial layers and decrease the strength of the resulting piezoelectric polarization electric field in the active region. Experimentally, use of an InGaN substrate serves to reduce the threading dislocation density in the epitaxial films, leading to decreased non-radiative recombination [31]–[37]. In this work, we show a monotonic increase in Γ_{e_hh} with increasing peak emission wavelength (λ_{peak}) within the red emission regime, from 26% at 555 nm to 57% at 858 nm, which

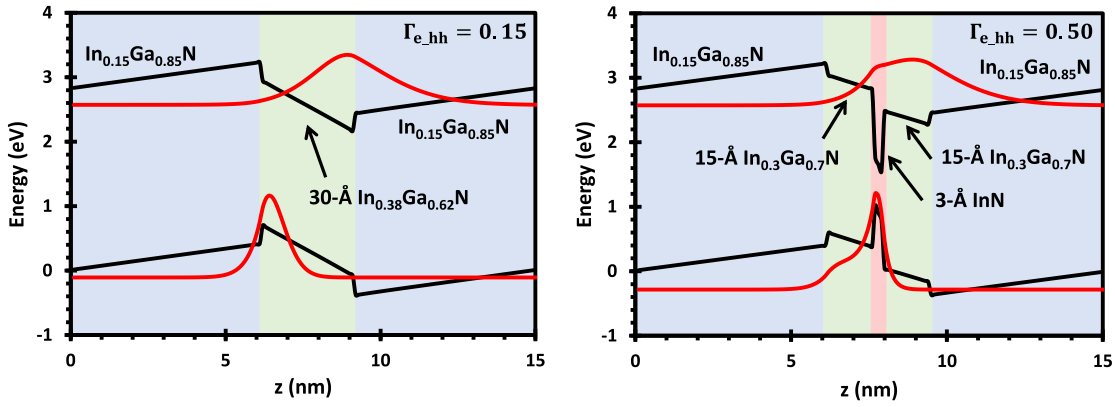

Fig. 1. Bandstructures and ground state wavefunctions in an $In_{0.15}Ga_{0.85}N/In_{0.38}Ga_{0.62}N$ QW (a) and an $In_{0.15}Ga_{0.85}N/In_{0.3}Ga_{0.7}N$/delta-InN QW with a 3 nm delta-layer (b), showing enhanced Γ_{e_hh} for the delta-InN structure.

we attribute to stronger localization of the electron-hole wavefunction to the center of the QW with increasing InN delta-layer thickness. The λ_{peak} of the $In_xGa_{1-x}N/In_yGa_{1-y}N$/delta-InN QW is tunable from ~555 nm–900 nm by varying the delta-layer thickness between 1 and 8 Å. We compare the optical properties of our $In_xGa_{1-x}N/In_yGa_{1-y}N$/delta-InN QW structure to an InGaN/InGaN QW (hereafter denoted as an $In_xGa_{1-x}N/In_yGa_{1-y}N$ QW where x represents the In-content in the barrier/substrate and y the In-content in the QW region), both with InGaN QBs, at the same λ_{peak}. Results show an R_{sp} enhancement of ~5–7x for $In_{0.15}Ga_{0.85}N/In_{0.3}Ga_{0.7}N$/delta-InN QWs with a 3 Å delta-InN layer when compared to a $In_{0.15}Ga_{0.85}N/In_{0.38}Ga_{0.62}N$ QW, with both emitting with λ_{peak} = 630 nm. These results are extremely promising and show that $In_xGa_{1-x}N/In_yGa_{1-y}N$/delta-InN QWs may be a superior alternative to GaN/InGaN QWs for high efficiency red emission.

2. Simulation Details

Band structure and wavefunction calculations were carried out using a self-consistent six-band $k \cdot p$ formalism developed by Chuang *et al.* [40]–[43]. A detailed description of the numerical model used in the script can be found in [19], and material parameters were obtained from [44] and [45]. The calculations for an $In_xGa_{1-x}N/In_yGa_{1-y}N$/delta-InN QW utilize a 60 Å $In_xGa_{1-x}N$ QB, 15 Å $In_yGa_{1-y}N$ sub-QW, and InN of variable thickness for the delta-QW, while a 60 Å $In_xGa_{1-x}N$ QB and 30 Å $In_yGa_{1-y}N$ QW were used for the $In_xGa_{1-x}N/In_yGa_{1-y}N$ QW. Numerical calculations account for all allowed transitions between available confined states in the conduction bands (CB) and valence bands (VB). Valence band mixing, strain effects, carrier screening, spin-orbit interactions, and spontaneous and piezoelectric polarization are considered. The model also accounts for the internal electrostatic fields which result from spontaneous and piezoelectric polarization, which arise due to lattice mismatch, with the details of the electric field calculation available in [19]. A carrier density (n) of 5×10^{18} cm^{-3} is used for most comparisons.

3. Results

Figs. 1(a) and (b) show the alignment of the energy band structure and electron and hole wavefunctions for an $In_{0.15}Ga_{0.85}N/In_{0.38}Ga_{0.62}N$ QW and an $In_{0.15}Ga_{0.85}N/In_{0.3}Ga_{0.7}N$/delta-InN QW with a 3 Å thick delta-layer, respectively. The energy bands shown in Fig. 1 are the first conduction subband ground state and the heavy hole (HH) ground state at zone center ($k = 0$). The energy band bending which is obvious in both of these band structures is a product of the

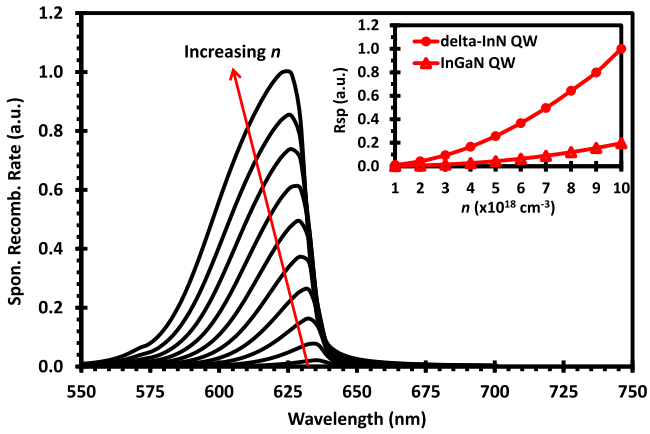

Fig. 2. Spontaneous recombination rate spectra for an $In_{0.15}Ga_{0.85}N/In_{0.3}Ga_{0.7}N$/delta-InN QW with a 3 Å delta-layer for $n = 1–10 \times 10^{18}$ cm^{-3}. Inset shows R_{sp} as a function of n for both the $In_{0.15}Ga_{0.85}N/In_{0.3}Ga_{0.7}N$/delta-InN QW with a 3 Å delta-layer and an $In_{0.15}Ga_{0.85}N/In_{0.38}Ga_{0.62}N$ QW which both have $\lambda_{peak} = 630$ nm at $n = 5 \times 10^{18}$ cm^{-3}.

piezoelectric and spontaneous polarization electric fields that exist within wurtzite GaN and InGaN. The strong electric fields which cause this band bending also serve to shift electrons and holes to opposite sides of the QW, leading to reduced Γ_{e_hh} and R_{sp} due to the QCSE. This effect is most pronounced in Fig. 1(a), in which the electron and hole wavefunctions are strongly localized to the CB minimum and VB maximum on opposite sides of the QW. As a consequence, the Γ_{e_hh} for this $In_{0.15}Ga_{0.85}N/In_{0.38}Ga_{0.62}N$ QW structure, which emits at 630 nm, is a mere 15%. Insertion of a 3 Å InN delta-layer into the center of an $In_{0.15}Ga_{0.85}N/In_{0.3}Ga_{0.7}N$ QW, as shown in Fig. 1(b), serves to localize the electron and hole wavefunctions to the center of the QW, increasing the Γ_{e_hh} to 50%, an improvement of nearly 3.5x. Calculations for conventional and delta-InN structures with GaN QBs and substrates, also emitting at 630 nm, show an Γ_{e_hh} of 10% for a conventional $GaN/In_xGa_{1-x}N$ QW and an Γ_{e_hh} of 18% for a $GaN/In_xGa_{1-x}N$/delta-InN QW. These enhancements demonstrate the effectiveness of using an InGaN substrate and InGaN QB layers, which lead to reduced interfacial lattice mismatch-based piezoelectric strain between epitaxial layers, which in turn reduces the electric field strength within the active region and improves Γ_{e_hh}. The use of $In_{0.15}Ga_{0.85}N$ QBs on an $In_{0.15}Ga_{0.85}N$ substrate allows for zero lattice mismatch between the barriers and the substrate. The lattice parameters of GaN, $In_{0.15}Ga_{0.85}N$, $In_{0.3}Ga_{0.7}N$, and $In_{0.38}Ga_{0.62}N$, are 3.189 Å, 3.242 Å, 3.296 Å, and 3.323 Å, respectively. In the case of GaN barriers, the lattice mismatch between the QBs and an $In_{0.3}Ga_{0.7}N$ sub-QW would be $\Delta a = 0.106$ Å, corresponding to an in-plane strain of $\varepsilon_{xx/yy} = 3.232\%$. For a $In_{0.38}Ga_{0.62}N$ QW with GaN QBs, the mismatch would be 0.135 Å, for a strain of $\varepsilon_{xx/yy} = 4.058\%$. By using an $In_{0.15}Ga_{0.85}N$ substrate and $In_{0.15}Ga_{0.85}N$ QBs, the lattice mismatch and corresponding in plane-strain for an $In_{0.3}Ga_{0.7}N$ sub-QW and an $In_{0.38}Ga_{0.62}N$ QW are reduced to 0.053 Å/1.616% and 0.082 Å/2.456%, respectively. This significant reduction in strain through use of an InGaN substrate and InGaN QBs is what allows for mitigation of the QCSE and improvement of Γ_{e_hh} by more than 3.5x.

Fig. 2 shows the spontaneous recombination rate spectra for an $In_{0.15}Ga_{0.85}N/In_{0.3}Ga_{0.7}N$/delta-InN structure with a 3 Å InN delta-layer for $n = 1–10 \times 10^{18}$ cm^{-3}. A semi-uniform increase in the recombination rate is observed with increasing n along with a slight blueshift of λ_{peak}. This blueshift can be attributed to increased carrier population in the QW, which forces some carriers to recombine with energies above that of the primary transition from states slightly above/below the CB and HH ground states. Although the spontaneous recombination rate spectra of the $In_{0.15}Ga_{0.85}N/In_{0.38}Ga_{0.62}N$ QW is not shown, it is important to point out that this structure exhibits a greater amount of blueshift than the $In_{0.15}Ga_{0.85}N/In_{0.3}Ga_{0.7}N$/delta-InN QW shown in Fig. 2.

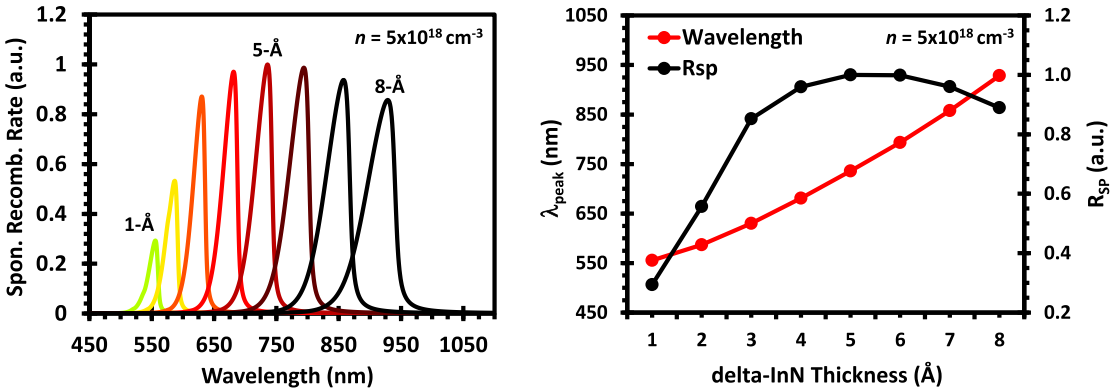

Fig. 3. (a) Spontaneous recombination rate spectra for $In_{0.15}Ga_{0.85}N/In_{0.3}Ga_{0.7}N$/delta-InN structures of varying delta-InN thickness for $n = 5 \times 10^{18}$ cm^{-3}. (b) $\lambda_{\rm peak}$ and R_{sp} as a function of delta-InN thickness.

The peak emission wavelength of the $In_{0.15}Ga_{0.85}N/In_{0.38}Ga_{0.62}N$ QW blueshifts by 19 nm when increasing n from 1×10^{18} to 10×10^{18} cm^{-3}, while the peak emission wavelength of the $In_{0.15}Ga_{0.85}N/In_{0.3}Ga_{0.7}N$/delta-InN QW only blueshifts by 13 nm. The inset of Fig. 2 plots the R_{sp} of an $In_{0.15}Ga_{0.85}N/In_{0.38}Ga_{0.62}N$ QW and an $In_{0.15}Ga_{0.85}N/In_{0.3}Ga_{0.7}N$/delta-InN QW with a 3 Å delta-layer as a function of n. A maximum R_{sp} enhancement of 6.8x is realized at $n = 1 \times 10^{18}$ cm^{-3}, with enhancement decreasing monotonically with increasing n to a value of 5.07x at $n = 1 \times 10^{19}$ cm^{-3}. This represents a substantial increase in radiative emission within the active region of the LED, which will lead to enhanced brightness and power efficiency.

Fig. 3(a) shows the spontaneous recombination rate spectra for delta-InN layers between 1 and 8 Å thick. Increasing the delta-InN thickness by only a single angstrom (less than one InN monolayer), produces a significant increase in $\lambda_{\rm peak}$. As the delta-layer thickness increases, confinement of energy states within the delta-layer decreases, allowing the CB and HH ground states to move closer to their theoretical minima/maxima, reducing the energy of the primary inter-band transition and increasing the emission wavelength as shown in Fig. 3(b). The Γ_{e_hh} increases with increasing delta-layer thickness up to a thickness of 6 Å, whereupon it begins to decrease as the delta-layer begins to behave more as an InN square well, with wavefunctions beginning to separate to opposite sides of InN delta-layer. This trend in Γ_{e_hh} is mirrored by a similar trend in R_{sp}, or the integral of each of the emission curves show in Fig. 3(a). R_{sp} also increases with increasing delta-layer thickness up to a thickness of 6 Å and decreases beyond it, illustrating the dependence of R_{sp} on Γ_{e_hh}, as shown in Fig. 3(b). While we have calculated the spectra for delta-layer thicknesses between 1 and 8 Å in increments of 1 Å, it is important to note that a single InN monolayer (ML) is approximately 3 Å thick [46]–[49]. While precision growth of single (3 Å) and double (6 Å) monolayers of InN has been demonstrated through use of both metal organic chemical vapor deposition (MOCVD) and molecular beam epitaxy (MBE) [46]–[49], the growth of InN fractional monolayers (FMLs), for example a 4 Å (4/3 ML) layer, is more difficult, as a variety of complex growth conditions effect the long- and short-range order of the incomplete top monolayer [47]–[49]. While Fig. 3 shows InN layers of fractional thickness (1, 2, 4, 5 Å, etc), it is important to note that our theoretical model does not make any accommodations for the additional morphologic complexity of FMLs, and treats these layers of fractional thickness as isotropic and continuous. Even assuming growth of InN FMLs to be reliably attainable, the emission peaks within the red emission regime are spaced by between 30 and 50 nm. For applications in which specific red wavelengths are desired, simply adjusting the InN delta-layer thickness would likely be insufficient to achieve precise emission wavelength targets.

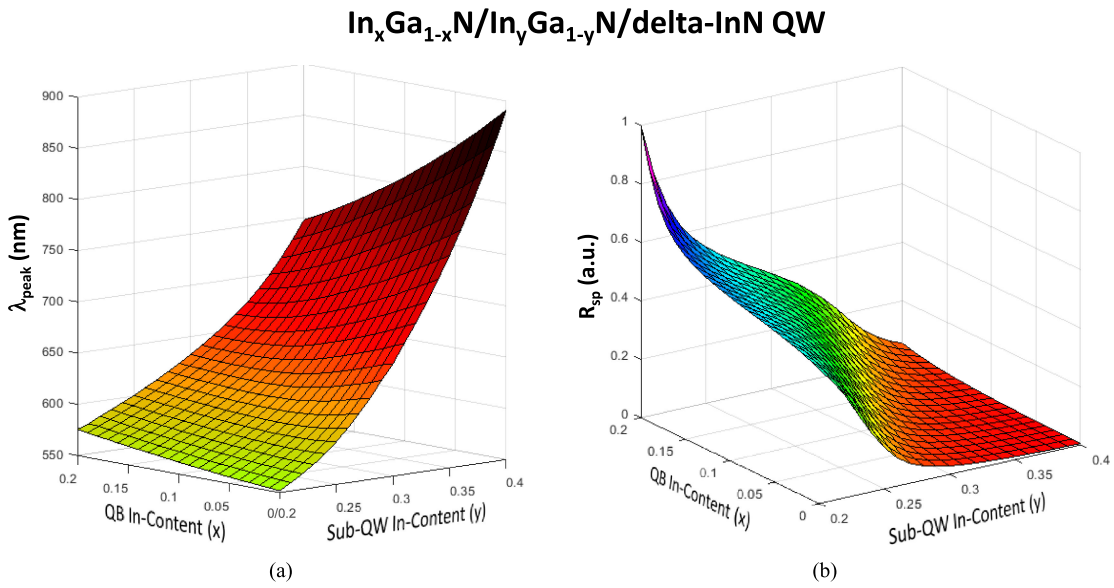

Fig. 4. (a) λ_{peak} dependence on the In-content of the QB and sub-QW regions for an $In_xGa_{1-x}N/In_yGa_{1-y}N$/delta-InN QW with a 3 Å delta-layer, showing that red emission wavelength is continuously tunable through small variations of the In-content in these regions. Chart colors are accurate. (b) R_{sp} dependence on the In-content in the QB and sub-QW regions.

Fig. 4(a) plots λ_{peak} as a function of the In-content in both the QB and sub-QW regions for an $In_xGa_{1-x}N/In_yGa_{1-y}N$/delta-InN QW with a 3 Å delta-layer at $n = 5 \times 10^{18}$ cm^{-3}. It is evident that λ_{peak} can be tuned continuously over a very large range through manipulation of the In-content in the $In_xGa_{1-x}N$ QB, $In_yGa_{1-y}N$ sub-QW, or both, for a fixed delta-layer thickness. This approach could allow for easy tuning of red LED λ_{peak} without the need to grow InN FMLs. A single 3 Å InN monolayer could be used, and the In-content in the QB and sub-QW regions could be tuned through alteration of the gas flow/atom flux rates during the MOCVD/MBE epitaxial growth process in order to achieve extremely precise emission wavelength targets. As shown in Fig. 4(a), engineering of the In-content in the $In_xGa_{1-x}N$ QB and $In_yGa_{1-y}N$ sub-QW can be used to vary λ_{peak} from green (550 nm) to the near-IR (890 nm). Fig. 4(b) plots R_{sp} for the same structure as a function of In-content in the QB and sub-QW regions. Combined, the data presented in these two figures shows that use of $In_xGa_{1-x}N/In_yGa_{1-y}N$/delta-InN QWs could allow for design of high-efficiency red LEDs. Fig. 4(b) also clearly illustrates the advantage of using InGaN in the substrate and QB, with R_{sp} increasing monotonically with In-content in the QB for all values of In-content in the sub-QW.

The large R_{sp} enhancements demonstrated through insertion of an InN delta-layer into the center of the InGaN QW translate directly to improvements in radiative recombination efficiency (η_{RAD}). Fig. 5(a) plots the η_{RAD} calculated using a simple ABC-model with Shockley-Read-Hall (SRH) and auger coefficients of 1x10^6 s^{-1} and 3.5 $\times$ 10^{-34} cm^{6}s^{-1} respectively [50]. The SRH and Auger coefficient values reported in [50] are taken from a variety of experimental and theoretical work, and are reasonable approximations for the materials used in our simulations. It is worthy of note that Auger coefficient value used here and reported in [50] is the theoretical value for InGaN, while the experimentally determined value may be as high as 1.4 $\times$ 10^{-30} cm^{6}s^{-1}. As expected, our $In_xGa_{1-x}N/In_yGa_{1-y}N$/delta-InN QW shows higher η_{RAD} than an $In_xGa_{1-x}N/In_yGa_{1-y}N$ QW emitting at 630 nm across a wide range of carrier densities. This enhancement can be attributed to the enhanced electron-hole wavefunction overlap facilitated by the InN delta-layer as previously described and shown in Fig. 1. Carrier injection efficiencies (η_{INJ}) were calculated for both structures as a function of n using the model described in [42]. The parameters used in this calculation were taken from [42]. Fig. 5(b) shows the η_{INJ} of each structure decreasing

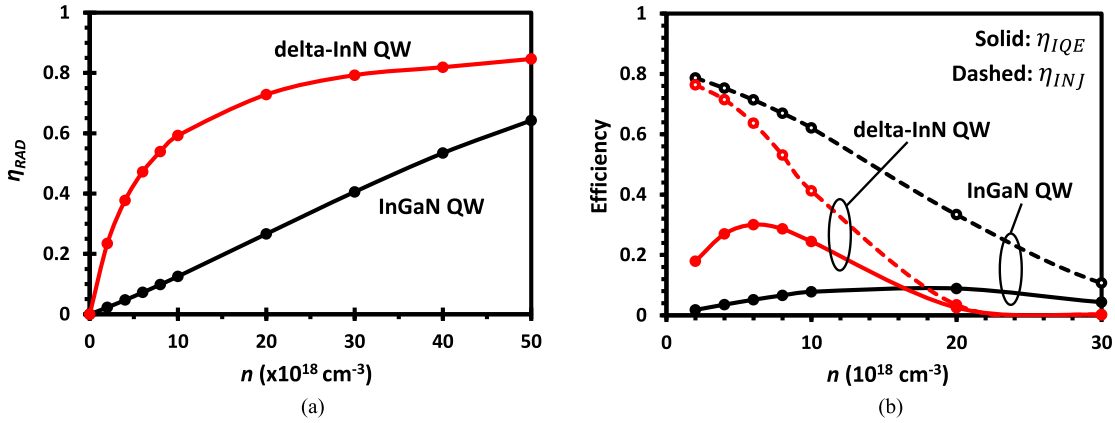

Fig 5. (a) η_{RAD}, and (b) η_{INJ} (dashed line) and η_{IQE} (solid line) for an $In_{0.15}Ga_{0.85}N/In_{0.38}Ga_{0.62}N$ QW (black) and an $In_{0.15}Ga_{0.85}N/In_{0.3}Ga_{0.7}N$/delta-InN QW with a 3 Å delta-layer QW (red) as a function of *n*. Both structures have $\lambda_{\text{peak}} \sim 630$ nm at $n = 5 \times 10^{18}$ cm^{-3}.

with increasing *n* due to increased carrier leakage from the QW at higher carrier densities (dashed lines). The η_{INJ} is higher for the $In_{0.15}Ga_{0.85}N/In_{0.38}Ga_{0.62}N$ QW at higher *n* due to its greater QB height of 0.29 eV, with the $In_{0.15}Ga_{0.85}N/In_{0.3}Ga_{0.7}N$/delta-InN QW having a barrier height of only 0.18 eV. As previously described, both structures were designed to emit at $\lambda_{\text{peak}} = 630$ nm at $n = 5 \times 10^{18}$ cm^{-3}, with the $In_{0.15}Ga_{0.85}N/In_{0.38}Ga_{0.62}N$ structure achieving this with an In-content 0.38 in the QW and the $In_{0.15}Ga_{0.85}N/In_{0.3}Ga_{0.7}N$/delta-InN structure with an In-content of 0.30 in the sub-QW. The greater band offset between the QB and QW regions in the $In_{0.15}Ga_{0.85}N/In_{0.38}Ga_{0.62}N$ structure makes it more resistant to carrier leakage when compared to the $In_{0.15}Ga_{0.85}N/In_{0.3}Ga_{0.7}N$/delta-InN structure. The solid lines in Fig. 5(b) plot the internal quantum efficiency (η_{IQE}), which is the product of η_{RAD} and η_{INJ}. Although the injection efficiency of the $In_xGa_{1-x}N/In_yGa_{1-y}N$/delta-InN structure is always lower than that of the $In_xGa_{1-x}N/In_yGa_{1-y}N$ QW, its η_{IQE} is significantly higher within the normal operating regime of LEDs ($n = 1$–10×10^{18} cm^{-3}) due to the massively enhanced η_{RAD} within this carrier density regime as shown in Fig. 5(a). The η_{IQE} of the $In_{0.15}Ga_{0.85}N/In_{0.3}Ga_{0.7}N$/delta-InN QW at $n = 2 \times 10^{18}$ cm^{-3} is 10x greater than that of the $In_{0.15}Ga_{0.85}N/In_{0.38}Ga_{0.62}N$ QW, with this enhancement decreasing linearly to 3.1x at $n = 1 \times 10^{19}$ cm^{-3}. At carrier densities in excess of $n = 2 \times 10^{19}$ cm^{-3} the η_{IQE} of the $In_xGa_{1-x}N/In_yGa_{1-y}N$/delta-InN structure falls below that of the $In_xGa_{1-x}N/In_yGa_{1-y}N$ QW. An electron blocking layer (EBL) could be possibly be used to reduce the carrier leakage of the delta-InN structure and improve its η_{INJ} at higher *n*.

It is also of great interest to investigate the potential of this $In_xGa_{1-x}N/In_yGa_{1-y}N$/delta-InN QW for laser applications. Fig. 6 shows the material gain for an $In_{0.15}Ga_{0.85}N/In_{0.38}Ga_{0.62}N$ QW and an $In_{0.15}Ga_{0.85}N/In_{0.3}Ga_{0.7}N$/delta-InN QW with a 3 Å delta-layer on $In_{0.15}Ga_{0.85}N$ substrates as a function of *n*. It has previously been shown that use of ternary InGaN substrates can dramatically improve the material gain and reduce the threshold carrier density of InGaN QW lasers emitting in the green and yellow emission regimes [27]. Here, our material gain calculations are based on Fermi's Golden Rule and a Lorentzian line-shape function [19], [27], [41]. Inhomogeneous broadening was not considered as no experimental data has been reported on inhomogeneous broadening for InGaN grown on ternary substrates [27]. The results shown in Fig. 6 indicate that the material gain and threshold carrier density of InGaN QW lasers emitting in the red emission regime can be enhanced through insertion of an InN delta-layer into the QW.

Fig. 6 shows that exceptional improvements in material gain can be realized through use of a delta-layer structure for lower *n*, with this enhancement becoming less pronounced as *n* increases. Assuming the threshold material gain to be approximately 1500 cm^{-1} [19], [51], we see that the threshold carrier density (n_{th}) is achieved around $n_{th} = 3\text{x}10^{19}$ cm^{-3} for the

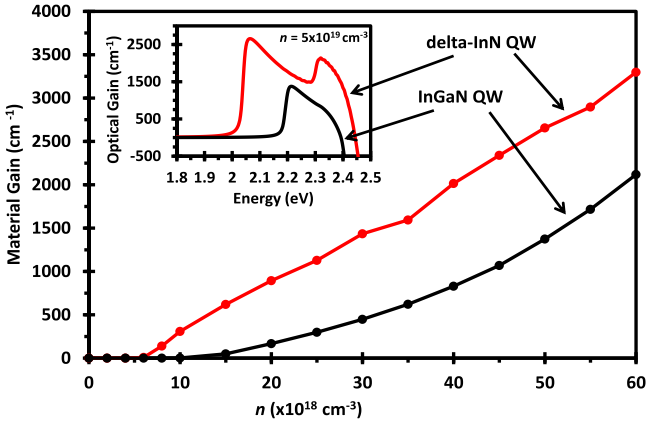

Fig. 6. Material gain as a function of n for an $In_{0.15}Ga_{0.85}N/In_{0.38}Ga_{0.62}N$ QW (black) and an $In_{0.15}Ga_{0.85}N/In_{0.3}Ga_{0.7}N$/delta-InN QW (red). Inset shows the optical gain spectra at $n = 5 \times 10^{18}$ cm^{-3}.

$In_{0.15}Ga_{0.85}N/In_{0.3}Ga_{0.7}N$/delta-InN QW (red), with the $In_{0.15}Ga_{0.85}N/In_{0.38}Ga_{0.62}N$ QW (black) having a material gain of less than 500 cm^{-1} at the same n. $n_{\rm th}$ is only achieved in the $In_{0.15}Ga_{0.85}N/In_{0.38}Ga_{0.62}N$ QW at a carrier density $n = 5 \times 10^{19}$ cm^{-3}. The inset of Fig. 6 shows the optical gain spectra of the $In_{0.15}Ga_{0.85}N/In_{0.3}Ga_{0.7}N$/delta-InN QW with a 3 Å delta-layer (red) and the $In_{0.15}Ga_{0.85}N/In_{0.38}Ga_{0.62}N$ QW (black) at $n = 5 \times 10^{19}$ cm^{-3}. The twin peaks present in the spectrum of the delta-layer structure are due to activation of a secondary interband transition which becomes available within the delta-layer once carrier density exceeds $n = 2 \times 10^{19}$ cm^{-3}. The effects of the secondary, higher energy peak at 2.32 eV can be eliminated through engineering of the laser cavity length. While both structures emit with $\lambda_{\rm peak} = 630$ nm (1.97 eV) at $n = 5 \times 10^{18}$ cm^{-3}, their optical gain spectra peak at shorter wavelengths of 602 nm (2.06 eV) and 561 nm (2.21 eV) for the $In_{0.15}Ga_{0.85}N/In_{0.3}Ga_{0.7}N$/delta-InN and $In_{0.15}Ga_{0.85}N/In_{0.38}Ga_{0.62}N$ QWs respectively. Just as $\lambda_{\rm peak}$ can be precisely tuned through manipulation of the In-content in the QB and sub-QW as shown in Fig. 4(a), the position of the primary peak in the optical gain spectra of an $In_xGa_{1-x}N/In_yGa_{1-y}N$/delta-InN QW can likewise be tuned for laser applications.

4. Conclusion

In summary, we have demonstrated for the first time that insertion of an InN delta-layer into an InGaN QW, along with use of an InGaN growth substrate, can produce unparalleled localization the electron and hole wavefunctions towards the center of the QW for red emission. This novel InGaN/InGaN/delta-InN QW produces significant improvements in Γ_{e_hh} and R_{sp} within the red emission regime, enabling high-efficiency red LEDs and laser diodes. Use of an InGaN growth substrate reduces the lattice mismatch experienced by epitaxial layers, reducing the magnitude of the spontaneous and piezoelectric electric fields and mitigating the QCSE in the active region. Analysis of structures emitting at a benchmark red emission wavelength of 630 nm shows an Γ_{e_hh} of 50% for a $In_{0.15}Ga_{0.85}N/In_{0.3}Ga_{0.7}N$/delta-InN structure on an InGaN substrate, compared to 15% for a $In_{0.15}Ga_{0.85}N/In_{0.38}Ga_{0.62}N$ QW on an InGaN substrate and 18% for a $In_{0.15}Ga_{0.85}N/In_{0.28}Ga_{0.72}N$/delta-InN QW on a GaN substrate. This enhanced Γ_{e_hh} increases R_{sp} by between ~5 - 7x within the carrier density range $n = 1\text{-}10 \times 10^{18}$ cm^{-3}, which in turn serves to enhance η_{IQE} by between 3 – 10x when compared to a $In_xGa_{1-x}N/In_yGa_{1-y}N$ QW emitting at the same wavelength. $\lambda_{\rm peak}$ can also be carefully tuned through manipulation of InN delta-layer thickness and In-content in the QB and sub-QW regions to achieve precise emission wavelength targets. Additionally, notable enhancements in material gain and $n_{\rm th}$ can also be achieved through use of an InN delta-layer making this structure of secondary interest for use in laser diodes. The

$In_xGa_{1-x}N/In_yGa_{1-y}N$/delta-InN QW structure grown on an InGaN substrate investigated in this work shows great promise for achieving high-efficiency InGaN LEDs and laser diodes emitting in the red spectral regime. This advancement could revolutionize the development of emitters for μLED displays and laser diodes by allowing for development of blue, green, *and* red pixel elements based on the same materials system.

References

[1] R. Arefin *et al.*, "III-N/Si3N4 integrated photonics platform for blue wavelengths," *IEEE J. Quantum Electron.*, vol. 56, no. 4, Aug. 2020, Art. no. 6300309.
[2] N. V. Trivino, R. Butte, J. Carlin, and N. Grandjean, "Continuous wave blue lasing in III-Nitride nanobeam cavity on silicon," *ACS Nanoletters*, vol. 15, pp. 1259–1263, 2015.
[3] L. A. Coldren, S. W. Corzine, and M. L. Masanovic, "Photonic integrated circuits," in *Diode Lasers and Photonic Integrated Circuits*. 2nd ed., Hoboken, NJ, USA: Wiley, 2012, ch. 8.
[4] S. Dussaigne *et al.*, "Full InGaN red light emitting diodes," *Appl. Phys. Lett.*, vol. 128, 2020, Art. no. 135704.
[5] J. Hwang, R. Hashimoto, S. Saito, and S. Nunoue, "Development of ingan-based red LED grown on (0001) polar surface," *Appl. Phys. Exp.*, vol. 7, 2014, Art. no. 071003.
[6] S. Zhang *et al.*, "Efficiency emission of ingan-based light-emitting diodes: Towards orange and red," *Photon. Res.*, vol. 8, no. 11, 2020.
[7] M. Philip, D. Choudhary, M. Djavid, K. Le, J. Paio, and H. Nguyen, High efficiency green/yellow and red InGaN/AlGaN nanowire light-emitting diodes grown by molecular beam epitaxy," *J. Sci.: Adv. Mater. Devices*, vol. 2, pp. 150–155, 2017.
[8] D. Iida, Z. Zhang, P. Kirilenko, M. Velazquez-Rizo, and K. Ohkawa, "Demonstration of low forward voltage ingan-based red LEDs," *Appl. Phys. Exp.*, vol. 13, 2020, Art. no. 031001.
[9] S. Pasayat *et al.*, "Demonstration of ultra-small ($<$10 μm) 632 nm red InGaN micro-LEDs with useful on-wafer external quantum efficiency ($>$0.2%) for mini-displays," *Appl. Phys. Exp.*, vol. 14, 2021, Art. no. 011004.
[10] C. M. Kang *et al.*, "Monolithic integration of algainp-based red and ingan-based green LEDs via adhesive bonding for multicolor emission," *Nat. Sci. Rep.*, vol. 7, 2017, Art. no. 10333.
[11] T. Frost *et al.*, "High performance red emitting multiple layer InGaN/GaN quantum dot laser," *Japanese J. Appl. Phys.*, vol. 55, 2016, Art. no. 032101.
[12] T. Frost, G. L. Su, A. Hazari, J. M. Dallesasse, and P. Bhattacharya, "Red and near-infrared III-Nitride quantum dot lasers," *IEEE J. Sel. Topics Quantum Electron.*, vol. 23, no. 6, Nov./Dec. 2017, Art. no. 1901409.
[13] M. E. Aumer, S. F. LeBoeuf, B. F. Moody, and S. M. Bedair, "Strain-induced piezoelectric field effects on light emission energy and intensity from AlInGaN/InGaN quantum wells," *Appl. Phys. Lett.*, vol. 79, 2001, Art. no. 3803.
[14] S. F. Chichibu *et al.*, "Impact of internal electric field and localization effect on quantum well excitons in AlGaN/GaN/InGaN light emitting diodes," *Physica Status Solidi*, vol. 183, no. 91, 2001.
[15] A. E. Aslanyan *et al.*, "Investigation into the internal electric-field strength in the active region of ingan/gan-Based LED structures and various number of quantum wells by electrotransmission spectroscopy," *Semiconductors*, vol. 54, no. 4, pp. 495–500, 2020.
[16] R. M. Farrell, D. A. Haeger, K. Fujito, S. P. DenBaars, S. Nakamura, and J. S. Speck, "Morphological evolution of InGaN/GaN light emitting diodes grown on free-standing m-plane GaN substrates," *J. Appl. Phys.*, vol. 113, 2013, Art. no. 063504.
[17] R. A. Arif, H. Zhao, Y. K. Ee, and N. Tansu, "Spontaneous emission and characteristics of staggered InGaN quantum-well light-emitting diodes," *IEEE J. Quantum Electron.*, vol. 44, no. 6, pp. 573–580, Jun. 2008.
[18] S. H. Park, D. Ahn, and J. W. Kim, "High-efficiency staggered 530 nm InGaN/InGaN/GaN quantum-well light emitting diodes," *Appl. Phys. Lett.*, vol. 94, 2009, Art. no. 041109.
[19] H. Zhao, R. A. Arif, Y. K. Ee, and N. Tansu, "Self-consistent analysis of strain-compensated InGaN-AlGaN quantum wells for laser and light-emitting diodes," *IEEE J. Quantum Electron.*, vol. 45, no. 1, pp. 66–78, Jan. 2009.
[20] S. H. Park, D. Ahn, B. H. Koo, and J. E. Oh, "Optical gain improvement in type-II InGaN/GaNSb/GaN quantum well structures composed of ingan/and gansb layers," *Appl. Phys. Lett.*, vol. 96, 2010, Art. no. 051106.
[21] L. Han, K. Kash, and H. Zhao, "Designs of blue and green light-emitting diodes based on type-II ingan-zngen2 quantum wells," *J. Appl. Phys.*, vol. 120, 2016, Art. no. 103102.
[22] J. Park and Y. Kawakami, "Photoluminescence property of InGaN single quantum well with embedded AlGaN δ layer," *Appl. Phys. Lett.*, vol. 88, 2006, Art. no. 202107.
[23] S. H. Park, J. Park, and E. Yoon, "Optical gain in InGaN/GaN quantum well structures with embedded AlGaN δ layer," *Appl. Phys. Lett.*, vol. 90, 2007, Art. no. 023508.
[24] H. Zhao, G. Liu, and N. Tansu, "Analysis of InGaN-delta-InN quantum wells for light-emitting diodes," *Appl. Phys. Lett.*, vol. 97, 2010, Art. no. 131114.
[25] S. Islam, V. Protasenko, S. Rouvimov, H. Xing, and D. Jena, "High-quality InN films on GaN using graded InGaN buffers by MBE," *Japanese J. Appl. Phys.*, vol. 55, 2016, Art. no. 05FD12.
[26] K. Wang, T. Kosel, and D. Jena, "Structural and transport properties of InN grown on GaN by MBE," *Physica Status Solidi C*, vol. 5, no. 6. pp. 1811–1814, 2008.
[27] J. Zhang and N. Tansu, "Optical gain and laser characteristics of InGaN quantum wells on ternary InGaN substrates," *IEEE Photon. J.*, vol. 5, no. 2, Apr. 2013, Art. no. 2600111.
[28] Y. K. Ooi and J. Zhang, "Design analysis of phosphor-free monolithic white light-emitting-diodes with InGaN/InGaN multiple quantum wells on ternary InGaN substrates," *AIP Adv.*, vol. 5, 2015, Art. no. 057168.

[29] J. Zhang and N. Tansu, "Improvement in spontaneous emission rates for InGaN quantum wells on ternary InGaN substrate for light-emitting diodes," *J. Appl. Phys.*, vol. 110, 2011, Art. no. 113110.
[30] S. H. Park, Y. T. Moon, J. S. Lee, H. K. Kwon, J. S. Park, and D. Ahn, "Spontaneous emission rate of green strain-compensated InGaN/InGaN LEDs using InGaN substrate," *Physica Status Solidi A*, vol. 208, no. 1, pp. 195–198, 2011.
[31] M. Shimizu, Y. Kawaguchi, K. Hiramatsu, and N. Sawaki, "MOVPE growth of thick homogeneous InGaN directly on sapphire substrate using AlN buffer layer," *Solid-State Electron.*, vol. 41, no. 2, pp. 145–147, 1997.
[32] D. Doppalapudi, S. N. Basu, K. F. Ludwig, and T. D. Moustakas, "Phase separation and ordering in InGaN alloys grown by molecular beam epitaxy," *J. Appl. Phys.*, vol. 84, 1998, Art. no. 1389.
[33] S. Chu *et al.*, "High-Quality InGaN films grown by hot-wall epitaxy with mixed (Ga+In) source," *Japanese J. Appl. Phys.*, vol. 28, pp. 427–429, 1999.
[34] T. L. Williamson *et al.*, "Highly luminescent InxGa1-xN thin films grown over the entire composition range by energetic neutral atom beam lithography & epitaxy (ENABLE)," *Physica Status Solidi C*, vol. 6, no. S2, pp. S409–S412, 2009.
[35] M. A. Hoffbauer *et al.*, "In-rich InGaN thin films: Progress on growth, compositional uniformity, and doping for device applications," *J. Vac. Sci. Technol. B*, vol. 31, 2013, Art. no. 03C114.
[36] T. Hirasaki *et al.*, "Growth of thick InGaN layers by tri-halide vapor phase epitaxy," *Japanese J. Appl. Phys.*, vol. 53, 2014, Art. no. 05FL02.
[37] T. Ohata, Y. Honda, M. Yamaguchi, and H. Amano, "Thick InGaN growth by metal organic vapor phase epitaxy with sputtered InGaN buffer layer," *Japanese J. Appl. Phys.*, vol. 52, 2013, Art. no. 08JB11.
[38] H. Wang *et al.*, "Investigation of the strain relaxation properties of InGaN layer and its effects on the InGaN structural and optical properties," *Physica B*, vol. 405, pp. 4668–4672, 2010.
[39] K. Pantzas *et al.*, "Semibulk ingan: A novel approach for thick, single phase, epitaxial InGaN layer grown by MOVPE," *J. Cryst. Growth*, vol. 370, pp. 57–62, 2013.
[40] S. L. Chuang and C. S. Chang, "k.p method for strained wurtzite semiconductors," *Phys. Rev. B*, vol. 54, no. 4, 1996.
[41] S. L. Chuang, "Optical gain of strained wurtzite GaN quantum-well lasers," *IEEE J. Quantum Electron.*, vol. 32, no. 10, pp. 1791–1800, Oct. 1996.
[42] S. L. Chuang and C. S. Chang, "A band-structure model of strained quantum-well wurtzite semiconductors," *Semicond. Sci. Technol.*, vol. 12, pp. 252–263, Art. no. 2997.
[43] S. L. Chuang, *Physics of Photonic Devices*, 2nd ed. New York, NY, USA: Wiley, 2009.
[44] I. Vurgaftman and J. R. Meyer, *Nitride Semiconductor Devices*. J. Piprek, Ed., Hoboken, NJ, USA: Wiley, 2007.
[45] I. Vurgaftman and J. R. Meyer, "Band parameters for nitrogen-containing semiconductors," *J. Appl. Phys.*, vol. 94, 2003, Art. no. 3675.
[46] S. Che, A. Yuki, H. Wantanabe, Y. Ishitani, and A. Yoshikawa, "Fabrication of asymmetric GaN/InN/InGaN/GaN quantum-well light emitting diodes for reducing the quantum-confined stark effect in the blue-green region," *Appl. Phys. Exp.*, vol. 2, 2009, Art. no. 021001.
[47] A. Yoshikawa *et al.*, "Proposal and achievement of novel structure InN/GaN multiple quantum wells consisting of 1 ML and fractional monolayer InN wells inserted in GaN matrix," *Appl. Phys. Lett.*, vol. 90, 2007, Art. no. 073101.
[48] A. Yoshikawa, S. B. Che, N. Hashimoto, H. Saito, Y. Ishitani, and X. Q. Wang, "Fabrication and characterization of novel monolayer InN quantum wells in a GaN matrix," *J. Vac. Sci. Technol. B*, vol. 25, no. 4, 2008.
[49] A. Yoshikawa, K. Kusakabe, N. Hashimoto, E. S. Hwang, D. Imai, and T. Itoi, "Systematic study on dynamic atomic layer epitaxy of InN on/in +c-GaN matrix and fabrication of fine-structure InN/GaN quantum wells: Role of high growth temperature," *J. Appl. Phys.*, vol. 120, 2016, Art. no. 225303.
[50] H. Zhao, G. Liu, J. Zhang, R. A. Arif, and N. Tansu, "Analysis of internal quantum efficiency and current injection efficiency in II-Nitride light-emitting diodes," *J. Display Technol.*, vol. 9, no. 4, 2013.
[51] H. Y. Ryu *et al.*, "High-Performance blue InGaN laser diodes with single-quantum-well active layers," *IEEE Photon. Technol. Lett.*, vol. 19, no. 21, pp. 1717–1719, Nov. 2007.